Increased mitochondrial mass in mitochondrial myopathy mice

Anna Wredenberg*, Rolf Wibom†, Hans Wilhelmsson*, Caroline Graff*, Heidi H. Wiener‡, Steven J. Burden‡, Anders Oldfors§, Håkan Westerblad¶, and Nils-Göran Larsson*‖

Departments of *Medical Nutrition and Biosciences and †Medical Laboratory Sciences and Technology, Karolinska Institute, Huddinge Hospital, S-141 86 Huddinge, Sweden; §Department of Pathology, Sahlgrenska Hospital, S-413 45 Göteborg, Sweden; ‡Skirball Institute for Molecular Medicine, New York University Medical Center, NY 10016; and ¶Department of Physiology and Pharmacology, Karolinska Institute, S-171 77 Stockholm, Sweden

Communicated by Rolf Luft, Karolinska Hospital, Stockholm, Sweden, October 1, 2002 (received for review June 24, 2002)

We have generated an animal model for mitochondrial myopathy by disrupting the gene for mitochondrial transcription factor A (*Tfam*) in skeletal muscle of the mouse. The knockout animals developed a myopathy with ragged-red muscle fibers, accumulation of abnormally appearing mitochondria, and progressively deteriorating respiratory chain function in skeletal muscle. Enzyme histochemistry, electron micrographs, and citrate synthase activity revealed a substantial increase in mitochondrial mass in skeletal muscle of the myopathy mice. Biochemical assays demonstrated that the increased mitochondrial mass partly compensated for the reduced function of the respiratory chain by maintaining overall ATP production in skeletal muscle. The increased mitochondrial mass thus was induced by the respiratory chain deficiency and may be beneficial by improving the energy homeostasis in the affected tissue. Surprisingly, *in vitro* experiments to assess muscle function demonstrated that fatigue development did not occur more rapidly in myopathy mice, suggesting that overall ATP production is sufficient. However, there were lower absolute muscle forces in the myopathy mice, especially at low stimulation frequencies. This reduction in muscle force is likely caused by deficient formation of force-generating actin–myosin cross bridges and/or disregulation of Ca^{2+} homeostasis. Thus, both biochemical measurements of ATP-production rate and *in vitro* physiological studies suggest that reduced mitochondrial ATP production might not be as critical for the pathophysiology of mitochondrial myopathy as thought previously.

The oxidative phosphorylation system consists of five enzyme complexes with a total of ≈80–100 subunits, and it produces the bulk part of the cellular ATP (1, 2). Skeletal muscle ATP is produced mainly by oxidative phosphorylation in slow-twitch (type I) fibers, whereas anaerobic sources such as glycolysis and phosphocreatine breakdown also are of importance in fast-twitch (type II) fibers.

The regulation of respiratory chain capacity is unique in its dual dependence on both the nuclear and mitochondrial genomes (1, 2). The mitochondrial DNA (mtDNA) is present in 10^3–10^4 copies per cell and encodes 13 proteins, which are critical subunits of the respiratory chain complexes I, III, IV, and V, as well as two ribosomal RNAs, and 22 transfer RNAs, which are necessary for mitochondrial protein synthesis (3). Nuclear genes encode the majority of the respiratory chain subunits and all protein components necessary for maintenance and expression of mtDNA.

Mutations of mtDNA cause several genetic syndromes in humans (1, 2) and are also implicated, through circumstantial evidence, in common age-associated diseases such as diabetes mellitus and Parkinson's disease and aging (4–6). Pathogenic mutations of mtDNA often impair mitochondrial protein synthesis and preferentially cause symptoms from highly aerobic postmitotic tissues, e.g., brain, skeletal muscle, and heart (1, 2). However, almost any organ can be affected, and the age of onset is variable (7). There is frequently heteroplasmy, i.e., a mixture of mutant and wild-type mtDNA, in the cells of affected patients. The levels of mutated mtDNA must exceed a certain minimal threshold to impair respiratory chain function, and affected patients often have widely varying levels of mutated mtDNA in different tissues. There is often a reasonably good correlation between the distribution of mutated mtDNA and clinical manifestations (1, 2). However, the molecular pathogenesis of mtDNA-mutation diseases has been debated intensely, because different mtDNA mutations, which have the common effect of impairing mitochondrial protein synthesis, often cause distinct clinical syndromes.

We have developed several mouse models for mtDNA-mutation disorders by using the *cre-loxP* recombination system to disrupt the nuclear gene for mitochondrial transcription factor A (*Tfam*) in selected tissue of the mouse (8–12). *Tfam* is ubiquitously expressed and absolutely required for mtDNA transcription (8, 13). Loss of *Tfam* causes depletion of mtDNA, loss of mitochondrial transcripts, loss of mtDNA-encoded polypeptides, and severe respiratory chain deficiency (8–12). This system allows spatial and some temporal control of the knockout and makes it possible to create respiratory chain deficiency in selected cell types of the mouse (8–12). Impaired mitochondrial translation or disruption of *Tfam* causes a global deficiency of all mtDNA-encoded respiratory chain subunits and thus the same type of respiratory chain deficiency affecting complexes I, III, IV, and V.

We now report characterization of a mouse with skeletal muscle-specific disruption of *Tfam* causing mitochondrial myopathy with ragged-red muscle fibers (RRFs), accumulation of abnormally appearing mitochondria, progressively deteriorating respiratory chain function, and reduced muscle-force production.

Materials and Methods

Breeding of Myopathy Mice. Mice with a knock-in of *cre* recombinase in the myosin light chain *1f* locus (*Mlc1f-cre*) of C57BL/6 background (14) were mated with $Tfam^{loxP}/Tfam^{loxP}$ mice of mixed genetic background (9, 15). Double-heterozygous offspring ($+/Tfam^{loxP}$, $+/Mlc1f\text{-}cre$) from this cross were identified and mated with $Tfam^{loxP}/Tfam^{loxP}$ mice. This latter mating produced four genotypes at the expected Mendelian frequencies of ≈25% each in a total of 209 genotyped mice: $Tfam^{loxP}/Tfam^{loxP}$, $+/Mlc1f\text{-}cre$ (25%); $Tfam^{loxP}/Tfam^{loxP}$ (26%); $+/Tfam^{loxP}$, $+/Mlc1f\text{-}cre$ (23%); and $+/Tfam^{loxP}$ (26%). The mean litter size was 7.7, which is in the normal range for the studied mouse strains. The tissue-specific knockout mice with the genotype $Tfam^{loxP}/Tfam^{loxP}$,+/Mlc-*cre*, hereafter referred to as "myopathy mice," thus had no increased embryonic or

Abbreviations: *Tfam*, mitochondrial transcription factor A; RRF, ragged-red muscle fiber; Mlc, myosin light chain; COX, cytochrome *c* oxidase; SDH, succinate dehydrogenase; SCR, succinate:cytochrome *c* reductase; CS, citrate synthase; MAPR, mitochondrial ATP-production rate; EDL, extensor digitorum longus.

‖To whom correspondence should be addressed. E-mail: nils-goran.larsson@mednut.ki.se.

www.pnas.org/cgi/doi/10.1073/pnas.232591499

neonatal lethality. Mice with the genotype $Tfam^{loxP}/Tfam^{loxP}$, hereafter referred to as "control mice," were used as controls and have been shown previously to have normal *Tfam* expression, normal mtDNA copy number, and normal respiratory chain function in different tissues (9).

PCR, Southern Blot, Northern Blot, and Western Blot Analysis. Determination of the *Tfam* genotype and detection of the *cre* transgene were performed by PCR analyses as described (8, 15). Skeletal muscle samples from myopathy mice ($n = 5–6$) and control mice ($n = 5–6$) were collected at 1, 2, and 4 months of age. The tissues were stored at −80°C until further use. Southern blot and Northern blot analyses were used to determine mtDNA and mtRNA copy number in DNA and RNA samples from skeletal muscle as described (8). Western blot analyses to determine *Tfam*, cytochrome *c* oxidase (COX) subunit II, and actin protein levels in skeletal muscle protein extracts were performed as described (8). Protein samples were boiled before loading the gel, which may lead to some aggregation of assembled COX subunits. A 12-aa residue peptide (MAYPFQLGLQDC) corresponding to a region of the highly conserved amino terminus of the COXII protein (16) was used to raise COXII antibodies. Preimmune sera from 10 rabbits were tested, and two that did not react with mouse total proteins were chosen for immunizations. A total of three injections with the peptide and adjuvant was given in selected rabbits, and serum was collected. Highly reactive antibodies were obtained after affinity purification of serum collected 2 weeks after the last immunization.

Morphologic Analysis. Muscle specimens were frozen in liquid nitrogen. Cryostat sections from the entire lower limb, the quadriceps femoris muscle, muscles from the back of the thigh, and extraocular muscles were analyzed by enzyme histochemistry to determine succinate dehydrogenase (SDH) activity (17), COX activity (18), or simultaneous COX and SDH activity (19). Cryostat sections were also stained with hematoxylin/eosin and modified Gomori trichrome. Specimens were fixed in 2.5% glutaraldehyde, postfixed in OsO_4, and embedded in Epon for electron microscopy. Ultrathin sections were contrasted with uranyl acetate and lead citrate (8).

Biochemical Evaluation of Respiratory Chain Function. Skeletal muscle samples from myopathy mice ($n = 4–5$) and control mice ($n = 4–5$) were collected at 1, 2, and 4 months of age. Mitochondria were isolated from skeletal muscle specimens (average weight, 76 mg with a range of 38–143 mg) from the hind limb. The respiratory chain enzyme activities of complexes I and III (NADH:cytochrome *c* reductase), complex I (NADH:coenzyme Q reductase), complexes II and III (succinate:cytochrome *c* reductase, SCR), complex IV (COX), and citrate synthase (CS) were determined as described (20). The respiratory chain enzyme and CS activities were determined at 35°C by using standard methods on a Delta automated photometer (Kone Instruments, Espoo, Finland). All activities were expressed as units per unit of CS activity in the mitochondrial suspension. The mitochondrial ATP-production rate (MAPR) in isolated mitochondria was determined with a firefly luciferase method at 25°C by using a 1251 luminometer (BioOrbit Oy, Turku, Finland; ref. 20). MAPR was determined with four different substrate combinations: glutamate + succinate (G + S), TMPD + ascorbate (T + A), palmitoyl-L-carnitine + malate (PC + M), and succinate + rotenone (S + R). Results from MAPR measurements were presented either as the ATP synthesis rate (units) per unit of CS activity (MAPR/CS) or per kilogram of skeletal muscle (mmol ATP/min/kg muscle, MAPR/kg).

Contractile Function. Intact fast-twitch extensor digitorum longus (EDL) and slow-twitch soleus muscles were isolated from control mice ($n = 5$) and myopathy mice ($n = 5$) at 3–3.5 months of age. Muscles were mounted in a chamber containing standard Tyrode solution and stimulated with brief current pulses as described (21). The force–frequency relationship was tested by producing contractions at 1-min intervals. The duration of contractions was 300 ms for EDL and 1 s for soleus, and frequencies tested ranged between 1 and 120 Hz and 1 and 100 Hz, respectively. Thereafter, fatigue was produced by tetanic contractions given with 2-s intervals. In total, 50 tetani were given in EDL (300-ms duration, 70 Hz) and 100 tetani in soleus (600-ms duration, 50 Hz). Finally, recovery was followed by producing the same type of tetanic contractions at 1, 2, 5, 10, 20, and 30 min after the end of fatiguing stimulation.

Statistical Analysis. Data are presented as mean ± SEM. A two-way ANOVA was used to analyze MAPR and enzyme activity data statistically. An unpaired *t* test was used to analyze all other data statistically.

Results

Progressive Inhibition of mtDNA Expression in Skeletal Muscle. The myopathy mice appeared healthy until the age of ≈3–4 months when reduced spontaneous activity was observed. This clinical phenotype progressed gradually, and the mice were killed at the age of ≈4–5 months because of weakness, markedly reduced spontaneous activity, and weight loss. The myopathy mice displayed a highly tissue-specific knockout pattern with presence of the *Tfam* knockout allele ($Tfam^{-}$) only in skeletal muscle as determined by PCR analyses (Fig. 1*A*). There were no detectable levels of Tfam protein in skeletal muscle specimens from 1-, 2-, and 4-month-old myopathy mice as determined by Western blot analyses (Fig. 1*C*). The apparent absence of Tfam protein at the age of 1 month demonstrates that efficient skeletal muscle-specific *Tfam* recombination has occurred before this age and is consistent with previous reports demonstrating that the Mlc1*f* promoter, which regulates *cre*-recombinase expression in skeletal muscle, is active from embryonic day 10 (22).

The levels of mtDNA were reduced in skeletal muscle of myopathy mice in comparison with control mice at the age of 1 month (mean ± SEM = 31 ± 3%; pairs of analyzed animals, $n = 6$), 2 months (36 ± 5%; $n = 7$), and 4 months (32%; $n = 2$), as demonstrated by Southern blot analyses (Fig. 1*B*). The mitochondrial transcript levels in myopathy mice were reduced at the age of 1 month (67 ± 4%; $n = 5$), 2 months (50 ± 5%; $n = 6$), and 4 months (30 ± 3%; $n = 6$), as determined by Northern blot analyses of skeletal muscle RNA (Fig. 1*B*). Consistent with the progressive reduction in mitochondrial transcript levels, the amounts of the mtDNA-encoded COXII protein were normal in myopathy mice at the age of 1 month, reduced to ≈50% at 2 months, and undetectable at 4 months of age, as determined by Western blot analyses of skeletal muscle protein extracts (Fig. 1*C*).

Morphologic and Biochemical Evidence for Increased Mitochondrial Mass. Morphologic analyses of muscle specimens from myopathy mice at different ages showed increased variability in muscle fiber size without signs of inflammation, necrosis, or increased interstitial connective tissue (Fig. 2 *A* and *D*). There were numerous RRFs (Fig. 2*B*), indicative of accumulation of mitochondria. Many of the RRFs were atrophic. Enzyme histochemical analysis of SDH activity showed accumulation of mitochondria in muscle fibers with evident COX deficiency (Fig. 2 *C* and *F*). This histochemical pattern of enzyme activities is typical for mitochondrial disease caused by impaired mtDNA expression because the catalytic subunits of COX are encoded by mtDNA, whereas SDH is exclusively nucleus-encoded (23). Ultrastructural analysis of skeletal muscle from myopathy mice confirmed the presence of increased mitochondrial mass, particularly in the subsarcolemmal region (Fig. 3). Many of the mitochondria were

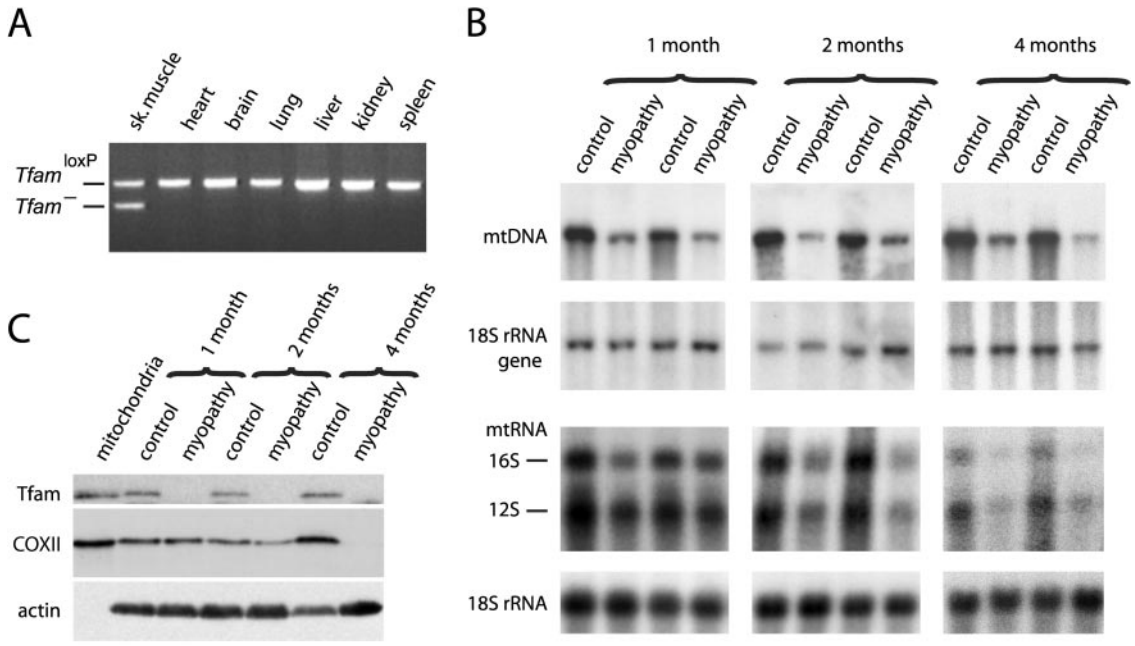

Fig. 1. Molecular characterization of skeletal muscle. (*A*) PCR analysis of tissue-specific recombination at the *Tfam* locus in different tissues from a myopathy mouse at 4 months of age. The knockout allele (*Tfam*$^{-}$) is present only in skeletal muscle. (*B*) Southern blot analysis to determine mtDNA levels (upper two panels) and Northern blot analysis to determine mtRNA levels (lower two panels) in skeletal muscle from myopathy and control mice at 1, 2, and 4 months of age. Membranes first were hybridized with an mtDNA probe and then rehybridized with an 18S rRNA gene fragment to control for loading. (*C*) Western blot analyses of *Tfam*, COXII, and actin protein levels in skeletal muscle of myopathy and control mice at 1, 2, and 4 months of age.

markedly enlarged with distorted cristae (Fig. 3*A*), but there were no paracrystalline inclusions. Ultrastructural analysis revealed no evidence of lipid accumulation in the respiratory chain-deficient skeletal muscle. The CS enzyme activity in homogenates of total skeletal muscle extracts reflects mitochondrial mass, and the CS activity was increased in myopathy mice of different ages (Fig. 4*A*).

Respiratory Chain Dysfunction and Decreased ATP-Production Rate. Biochemical measurements demonstrated a progressive reduction of respiratory chain enzyme activities in skeletal muscle of myopathy mice (Fig. 4*B*) consistent with the observed progressive reduction in mtDNA expression (Fig. 1 *B* and *C*). The activities of respiratory chain enzyme complexes containing mtDNA-encoded subunits were reduced, whereas the activity of SCR, which includes complex II and III, was almost unaffected (Fig. 4*B*). It should be noted that the *in vitro* activity of complex II is much lower than that of complex III, and the SCR activity therefore mainly reflects the complex II activity. The MAPR/CS in skeletal muscle of myopathy mice (Fig. 4*C*) was reduced with substrates entering at the level of complex I and II (G+S) or complex IV (T+A) but normal with

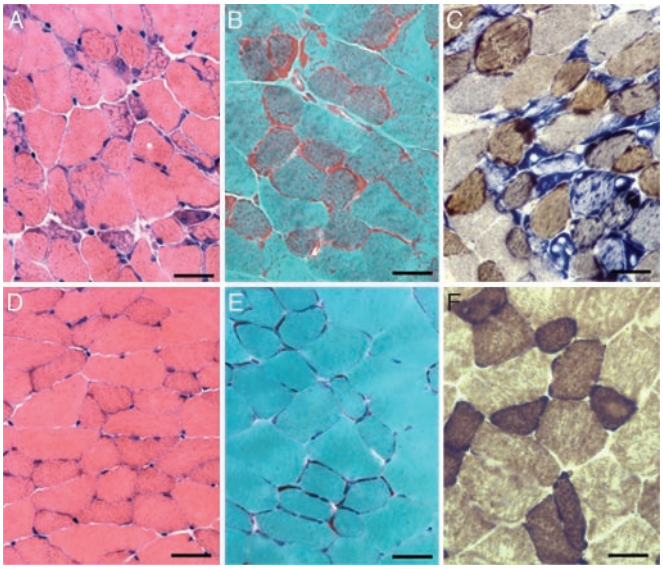

Fig. 2. Morphological analysis of skeletal muscle. Analysis of tissue sections from EDL muscle from a myopathy (*A–C*) and a control (*D–F*) mouse at 3 months of age. (Scale bar, 25 μm.) (*A* and *D*) Hematoxylin/eosin staining. There are scattered atrophic fibers in the myopathy mouse. (*B* and *E*) Modified Gomori trichrome staining. There are numerous RRFs in the myopathy mouse. (*C* and *F*) Staining to detect simultaneous COX/SDH activity. The muscle fibers that appear blue in the myopathy mouse are COX-deficient and contain accumulation of mitochondria.

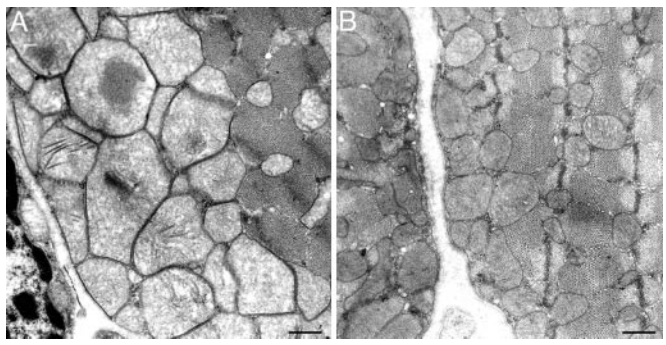

Fig. 3. Electron microscopy studies of skeletal muscle. Electron micrographs of ultrathin sections from the tibialis anterior muscle of a myopathy mouse (*A*) and a control mouse (*B*) are depicted. (Scale bar, 2 μm.) There is marked accumulation of enlarged mitochondria in skeletal muscle, particularly in the subsarcolemmal region, of the myopathy mouse.

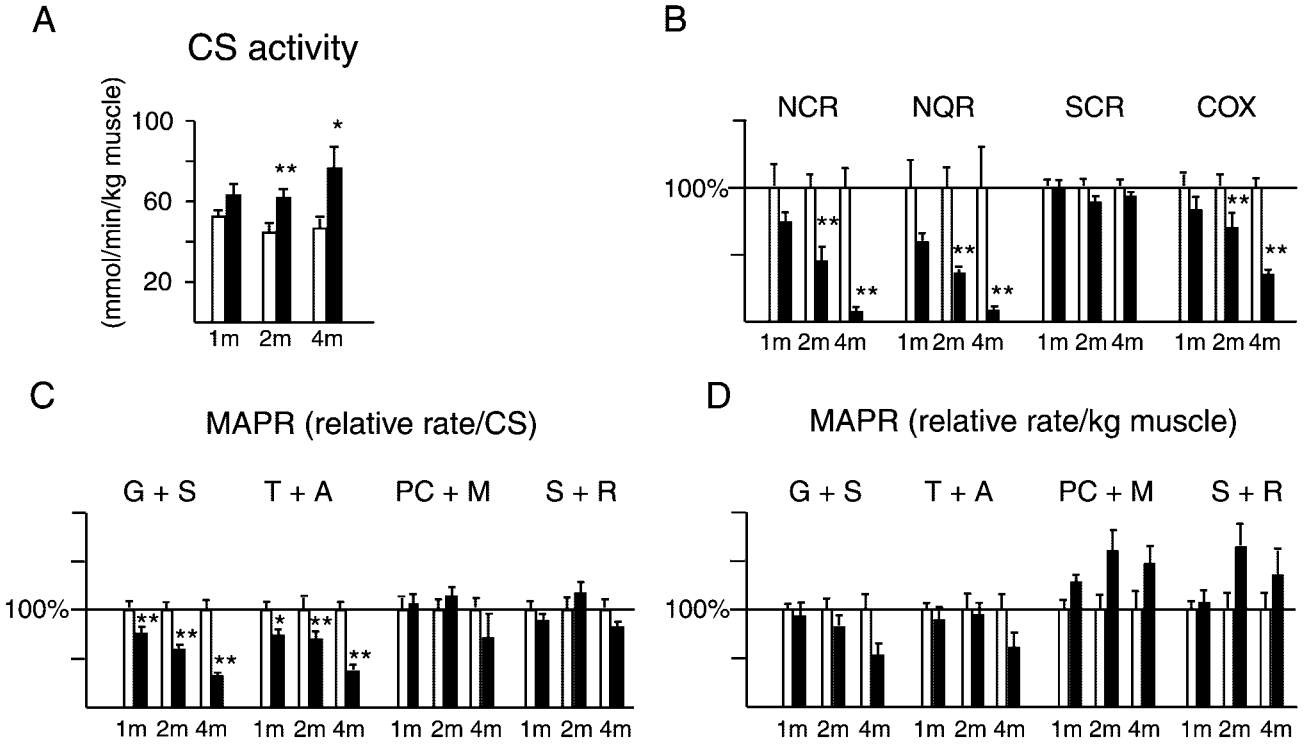

Fig. 4. Biochemical measurements of the respiratory chain function in skeletal muscle. The results from biochemical measurements in skeletal muscle from myopathy (M, black bars) and control (C, white bars) mice at 1 month (1m), 2 months (2m), and 4 months (4m) of age are shown. The bars indicate mean ± SEM, and the asterisks indicate statistical significance (*, $P < 0.05$; **, $P < 0.01$). (*A*) CS activity in mmol/min/kg of muscle. (*B*) Relative enzyme activities of respiratory chain enzyme complexes I and III (NADH cytochrome *c* reductase, NCR), complex I (NADH coenzyme Q reductase, NQR), complexes II and III (SCR), and complex IV (COX). The relative enzyme activities presented as 100% in the figure correspond to the following absolute ratios of enzyme activities per unit of CS activity at 1, 2, and 4 months of age, respectively: NCR, 1.10, 0.83, and 1.19; NQR, 0.27, 0.22, and 0.24; SCR, 0.68, 0.69, and 0.55; COX, 1.82, 1.97, and1.94. (*C*) Results from measurements of the MAPR per unit of CS activity. The relative MAPR/CS presented as 100% in the figure corresponds to the following absolute ratios of MAPR per unit of CS activity at 1, 2, and 4 months of age, respectively: glutamate + succinate (G + S), 0.30, 0.35, and 0.33; TMPD + ascorbate (T + A), 0.26, 0.29, and 0.29; palmitoyl-L-carnitine + malate (PC + M), 0.07, 0.07, and 0.06; succinate + rotenone (S + R), 0.06, 0.06, and 0.06. (*D*) Results from measurements of MAPR per kg of muscle. The relative MAPR per kg presented as 100% in the figure corresponds to the following absolute ratios of MAPR per kg of skeletal muscle (mmol ATP/min/kg muscle) at 1, 2, and 4 months of age, respectively: G + S, 15.4, 15.5, and 15.6; T + A, 13.6, 13.0, and 13.6; PC + M, 3.72, 3.12, and 2.95; S + R, 3.22, 2.60, and 2.88.

substrates entering at the level of complex II (S + R) or through fatty acid oxidation (PC + M). Interestingly, MAPR/CS was generally more decreased than the MAPR/kg of skeletal muscle in myopathy mice (Fig. 4*D*), which is consistent with the suggestion that the increased mitochondrial mass partly compensates for the respiratory chain deficiency.

Decreased Absolute Muscle Force. Weight and length of EDL and soleus muscles were similar in myopathy and control mice. The EDL muscle of myopathy mice displayed shorter contraction times and shorter twitch-relaxation times (Table 1). There were no significant differences in speed of contraction and relaxation in soleus muscle between myopathy and control mice (Table 1). EDL muscle from myopathy mice produced lower absolute forces between 20 and 120 Hz, and the force–frequency relationship was shifted to the right (Fig. 5 *A* and *B*). The force decline during fatiguing stimulation of EDL muscle from myopathy and control mice was similar (Fig. 5*E*), whereas the mean force during recovery was somewhat higher in EDL muscle from myopathy mice (Fig. 5*F*). Soleus muscle from myopathy mice

Table 1. Measurements of contraction and relaxation times in isolated skeletal muscles of myopathy and control mice at 3–3.5 months of age

	EDL		Soleus	
	Myopathy mice	Control mice	Myopathy mice	Control mice
Twitch				
Contraction time, ms	23.4 ± 1.2	30.2 ± 1.6*	65.4 ± 11.9	69.8 ± 4.6
Half-relaxation time, ms	20.2 ± 1.5	33.0 ± 3.7**	127.4 ± 36.6	91.2 ± 10.4
Tetanus				
Half-contraction time, ms	36.4 ± 3.1	44.6 ± 1.5**	99.0 ± 17.1	73.4 ± 3.5
Half-relaxation time, ms	37.2 ± 0.7	37.4 ± 2.3	137.4 ± 18.1	134.0 ± 14.3

All values are presented as mean ± SEM. Significant differences between myopathy and control mice are indicated by asterisks (*, $P < 0.01$; **, $P < 0.05$). Tetanic measurements were performed on 120- and 100-Hz tetani in EDL and soleus muscles, respectively.

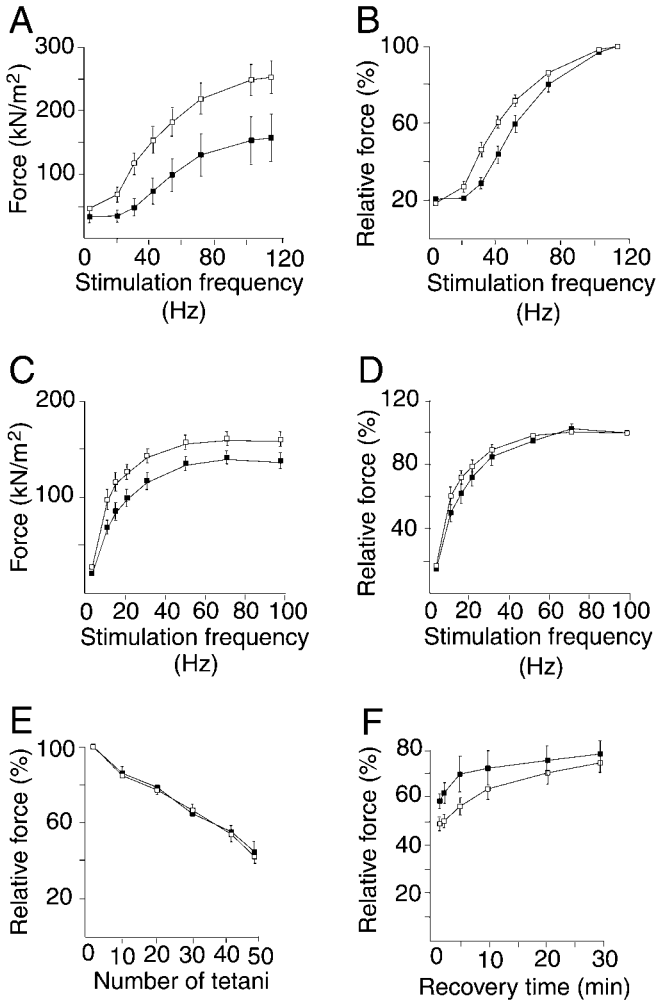

Fig. 5. Contractile function of skeletal muscle. Contractile parameters were assessed by *in vitro* studies of skeletal muscle from myopathy (filled symbols) and control (open symbols) mice at the age of 3–3.5 months. (*A* and *B*) The force–frequency relationship in EDL muscle. The absolute forces generally were lower and the force–frequency relationship was shifted to the right in myopathy mice. (*C* and *D*) The force–frequency relationship in soleus muscle. The forces generally were lower and the force–frequency relationship was slightly shifted to the right in myopathy mice. (*E*) Force production during fatiguing stimulation of EDL. (*F*) Force production during recovery of EDL.

produced significantly lower absolute forces between 10 and 50 Hz (Fig. 5*C*), and there was a slight rightward shift of the force–frequency relationship (Fig. 5*D*). There were no significant differences in force production during fatigue and recovery in soleus muscles between control and myopathy mice (data not shown).

Discussion

We have generated myopathy mice with selective disruption of mtDNA gene expression in skeletal muscle. These tissue-specific knockout animals reproduce important pathophysiological features found in human patients with mitochondrial myopathy, i.e., RRFs with COX deficiency (1), accumulation of abnormally appearing mitochondria (23), and progressively deteriorating respiratory chain function in skeletal muscle (24, 25). Thus it can be concluded that important morphological hallmarks of mitochondrial myopathy are a direct consequence of impaired mtDNA gene expression. We previously generated other tissue-specific *Tfam* knockouts with disruption of respiratory chain function in cardiomyocytes (9, 10), pancreatic beta cells (11), and cortical neurons (12). These mouse models have reproduced important phenotypes of human mitochondrial disease, e.g., dilated cardiomyopathy (9, 10), atrioventricular heart conduction blocks (9, 10), diabetes mellitus caused by deficient glucose-stimulated insulin release (impaired stimulus-secretion coupling in pancreatic beta cells; ref. 11), and spontaneous or stress-induced neuronal cell death (12). The tissue-specific *Tfam* knockouts thus have clarified that pathophysiology events downstream of the respiratory chain deficiency are sufficient to generate a variety of organ-specific manifestations in mitochondrial disease.

The myopathy mice had undetectable levels of Tfam protein in skeletal muscle at the age of 1 month and developed a progressive reduction of mtDNA expression and respiratory chain enzyme activities between the ages of 1 and 4 months. These findings are in line with observations from other tissue-specific *Tfam* knockout mice demonstrating a period of weeks (9–11) to months (12) between disruption of *Tfam* and the occurrence of severe respiratory chain deficiency. This time lag is likely determined by turnover rates for *Tfam* transcripts, Tfam protein, mtDNA, mitochondrial transcripts, and mtDNA-encoded respiratory chain subunits. We previously showed that mice with a moderate reduction of mtDNA copy number have normal levels of several mtDNA-encoded transcripts and proteins consistent with up-regulation of mitochondrial RNA and protein stability (8). Furthermore, studies of cell lines have shown that inhibition of mtDNA expression dramatically increases the stability of mtDNA-encoded transcripts and proteins (26, 27).

A particularly striking similarity to human disease was the abundance of RRFs with COX deficiency in the myopathy mice. RRFs are commonly found in skeletal muscle of patients with impaired mitochondrial translation caused by deletions or point mutations of mitochondrial tRNA genes. The RRFs are skeletal muscle fiber segments that contain accumulations of abnormal mitochondria and therefore stain red with modified Gomori trichrome. The abundant mitochondria in RRFs are often COX-deficient, suggesting that the respiratory chain deficiency is associated directly with the increased mitochondrial mass. Mitochondrial content in skeletal muscle has been shown to alter in response to changes in functional demands. Increased mitochondrial volume density has been detected after endurance exercise (28, 29) and in regenerating skeletal muscle (30). Enzyme histochemistry, electron micrographs, and CS activity assays demonstrated that there was a substantial increase in mitochondrial mass in the myopathy mice. The myopathy mice displayed a severe reduction of MAPR/CS, whereas the MAPR/kg was less affected. This indicates that the increased mitochondrial mass partly compensates for the reduced function of the respiratory chain by maintaining overall ATP production in skeletal muscle of the myopathy mice. The increased mitochondrial mass is thus a secondary response to the respiratory chain deficiency and may be beneficial by improving the energy homeostasis in the affected tissue.

Force measurements demonstrated that the EDL muscle was more affected than the soleus muscle. EDL muscles are composed mainly of fast-twitch (type II) fibers, whereas soleus muscles of the mouse strains we used contain roughly equal amounts of slow-twitch (type I) and type II fibers (data not shown). The majority of the respiratory chain-deficient muscle fibers were type II fibers (data not shown) as expected because the Mlc1*f* promoter, regulating *cre*-recombinase expression in the myopathy mouse, is active mainly in type II muscle fibers. Surprisingly, fatigue development did not occur more rapidly in *Tfam* knockout muscles, suggesting that decreased mitochondrial ATP production is not a critical factor. It should be noted that fatigue induced by repeated tetanic contractions

depends on respiratory chain function, because acute cyanide exposure markedly accelerates fatigue development (31). There were lower absolute muscle forces in the myopathy mice, especially at low stimulation frequencies. This reduction in muscle force is likely caused by deficient formation of force-generating actin–myosin cross bridges and/or disregulation of Ca^{2+} homeostasis (32). Thus, both biochemical measurements of MAPR and *in vitro* physiological studies suggest that reduced mitochondrial ATP production might not be as critical for the pathophysiology of mitochondrial myopathy as thought previously. This interesting question will have to be addressed in future studies investigating alternate pathophysiological mechanisms such as excessive reactive oxygen species formation and altered intracellular Ca^{2+} regulation.

We thank Ewa Gustavsson for technical assistance with the biochemical assays. A.W. is supported by an M.D.–Ph.D. fellowship from Karolinska Institute; H. Wilhelmsson is supported by Stiftelsen Frimurare Barnhuset i Stockholm and Stiftelsen Sven Jerrings Fond; H. Westerblad is supported by Swedish Research Council Project 10842 and 14402; and N.-G.L. is supported by the Swedish Research Council, Funds of Karolinska Institute, the Torsten and Ragnar Söderberg Foundations, the Swedish Heart and Lung Foundation, and the Swedish Foundation for Strategic Research (Functional Genomics). S.J.B. is supported by National Institutes of Health Grant NS27963. A.O. is supported by Swedish Research Council Project 7122.

1. Larsson, N. & Clayton, D. (1995) *Annu. Rev. Genet.* **29,** 151–178.
2. Smeitink, J., van Den Heuvel, L. & DiMauro, S. (2001) *Nat. Rev. Genet.* **2,** 342–352.
3. Anderson, S., Bankier, A. T., Barell, B. G., deBruijn, M. H. L., Coulson, A. R., Drouin, J., Eperon, I. C., Nierlich, D. P., Roe, B. A., Sanger, F., *et al.* (1981) *Nature* **290,** 457–465.
4. Larsson, N.-G. & Luft, R. (1999) *FEBS Lett.* **455,** 199–202.
5. Wallace, D. C. (1992) *Science* **256,** 628–632.
6. Wallace, D. C. (1999) *Science* **283,** 1482–1488.
7. Munnich, A. & Rustin, P. (2001) *Am. J. Med. Genet.* **106,** 4–17.
8. Larsson, N.-G., Wang, J., Wilhelmsson, H., Oldfors, A., Rustin, P., Lewandoski, M., Barsh, G. S. & Clayton, D. A. (1998) *Nat. Genet.* **18,** 231–236.
9. Wang, J., Wilhelmsson, H., Graff, C., Li, H., Oldfors, A., Rustin, P., Brüning, J. C., Kahn, C. R., Clayton, D. A., Barsh, G. S., Thoren, P. & Larsson, N.-G. (1999) *Nat. Genet.* **21,** 133–137.
10. Li, H., Wang, J., Wilhelmsson, H., Hansson, A., Thoren, P., Duffy, J., Rustin, P. & Larsson, N.-G. (2000) *Proc. Natl. Acad. Sci. USA* **97,** 3467–3472.
11. Silva, J. P., Kohler, M., Graff, C., Oldfors, A., Magnuson, M. A., Berggren, P. O. & Larsson, N.-G. (2000) *Nat. Genet.* **26,** 336–340.
12. Sorensen, L., Ekstrand, M., Silva, J. P., Lindqvist, E., Xu, B., Rustin, P., Olson, L. & Larsson, N.-G. (2001) *J. Neurosci.* **21,** 8082–8090.
13. Falkenberg, M., Gaspari, M., Rantanen, A., Trifunovic, A., Larsson, N.-G. & Gustafsson, C. M. (2002) *Nat. Genet.* **31,** 289–294.
14. Bothe, G. W., Haspel, J. A., Smith, C. L., Wiener, H. H. & Burden, S. J. (2000) *Genesis* **26,** 165–166.
15. Ekstrand, M. & Larsson, N.-G. (2002) *Methods Mol. Biol.* **197,** 391–400.
16. Michael, N. L., Rothbard, J. R., Shiurba, R. A., Linke, H. K., Schoolnik, G. K. & Clayton, D. A. (1984) *EMBO J.* **3,** 3165–3175.
17. Dubowitz, V. & Brooke, M. (1973) *Muscle Biopsy: A Modern Approach* (Saunders, London).
18. Seligman, A. M., Karnovsky, M. J., Wasserkrug, H. L. & Hanker, J. S. (1969) *J. Cell Biol.* **38,** 1–14.
19. Petruzzella, V., Moraes, C. T., Sano, M. C., Bonilla, E., DiMauro, S. & Schon, E. A. (1994) *Hum. Mol. Genet.* **3,** 449–454.
20. Wibom, R., Hagenfeldt, L. & Döbeln, U. v. (2002) *Anal. Biochem.*, in press.
21. Dahlstedt, A. J., Katz, A., Wieringa, B. & Westerblad, H. (2000) *FASEB J.* **14,** 982–990.
22. Lyons, G. E., Ontell, M., Cox, R., Sassoon, D. & Buckingham, M. (1990) *J. Cell Biol.* **111,** 1465–1476.
23. Larsson, N.-G. & Oldfors, A. (2001) *Acta Physiol. Scand.* **171,** 385–393.
24. Larsson, N.-G., Holme, E., Kristiansson, B., Oldfors, A. & Tulinius, M. (1990) *Pediatr. Res.* **28,** 131–136.
25. Larsson, N.-G., Tulinius, M. H., Holme, E., Oldfors, A., Andersen, O., Wahlström, J. & Aasly, J. (1992) *Am. J. Hum. Genet.* **51,** 1201–1212.
26. England, J. M., Costantino, P. & Attardi, G. (1978) *J. Mol. Biol.* **119,** 455–462.
27. Lansman, R. A. & Clayton, D. A. (1975) *J. Mol. Biol.* **99,** 761–776.
28. Holloszy, J. O. & Booth, F. W. (1976) *Annu. Rev. Physiol.* **38,** 273–291.
29. Holloszy, J. O. & Coyle, E. F. (1984) *J. Appl. Physiol*. **56,** 831–838.
30. Duguez, S., Feasson, L., Denis, C. & Freyssenet, D. (2002) *Am. J. Physiol.* **282,** E802–E809.
31. Lannergren, J. & Westerblad, H. (1991) *J. Physiol. (London)* **434,** 307–322.
32. Westerblad, H. & Allen, D. G. (1996) *Acta Physiol. Scand.* **156,** 407–416.